Two-component model for the associated multiplicity in inclusive reactions*

J. L. Alonso† and A. C. D. Wright‡
Stanford Linear Accelerator Center, Stanford University, Stanford, California 94305
(Received 28 April 1975)

We present a simple, two-component model for the charged multiplicity associated with the observed particle in an inclusive reaction. At small p_T the scattering is ascribed to a coherent or "soft" component, whereas at large p_T the production mechanism is assumed to be incoherent or "hard." At fixed incident energy and missing mass, the p_T dependence of $\bar{n}_c$ is given by the relative weights of hard and soft scattering, so that the multiplicity is a sensitive probe of the transition region between the two components. The model is applied to recent multiplicity data for $pp \to pX$ and $pp \to \pi^+ X$ at 28.5 GeV/c, as well as to data at Fermilab and CERN-ISR energies.

I. INTRODUCTION

One facet of recent experimental work on inclusive reactions has been the study of the mean total charged multiplicity $\bar{n}_c$ associated with the observed trigger particle.[1] At CERN-ISR energies,[2] results obtained for $pp \to \pi^0 X$ at 90° in the c.m. system show that $\bar{n}_c$ rises roughly linearly with increasing transverse momentum in the range $1 \lesssim p_T \lesssim 4$ GeV/c (since $\theta = 90°$, this could be interpreted as a linear dependence on $|\vec{p}_3|$, the momentum of the observed particle). At Fermilab, multiplicity data[3] for $pp \to pX$ at 205 GeV/c show little or no p_T dependence for $0 \lesssim p_T \lesssim 1$ GeV/c when M^2 is fixed, where M^2 is the mass squared of X. Finally, the Brookhaven-Purdue-VPI (BPV) collaboration[4,5] has measured $\bar{n}_c$ as a function of p_T for various fixed values of the missing mass. For $pp \to pX$ the associated multiplicity is approximately independent of p_T except for a rise of $\Delta\bar{n}_c \approx 0.6$ charged particles over an interval of $\Delta p_T \approx 0.4$–0.6 GeV/c. The location of the rise moves towards smaller values of p_T with increasing missing mass. The corresponding data for $pp \to \pi^+ X$ are relatively meager, but are consistent with a behavior similar to that obtained when a proton is the trigger particle.

Several authors[6-10] have proposed models to explain these results, particularly the preliminary BPV data.[4] In the bremsstrahlung model of Ref. 6 it is not clear how to treat $pp \to \pi^+ X$, and in the multiple-quark-scattering model of Ref. 7 the position of the rise does not move with missing mass. In multicomponent[8] and multiperipheral-bremsstrahlung[9] models the rise in multiplicity does not appear to be confined to a restricted interval in p_T, whereas a pure multiperipheral description[10] provides a multiplicity which is only weakly dependent on p_T for fixed missing mass.

In the present work we interpret multiplicity and cross-section data in terms of a simple, two-component model for inclusive reactions. At fixed energy the multiplicity associated with each component depends only on the missing mass, so there is no explicit p_T dependence. However, in the kinematic transition region, where the two components are of comparable importance, $\bar{n}_c$ may be p_T-dependent at fixed missing mass.

To be more specific, we assume that production at large p_T results from a "hard" interaction.[11] That is, the interaction is local and incoherent, and the inclusive cross section is characterized by a power-law dependence on p_T^2. Several models[11] share this hard-scattering property; in particular, for the hard component we shall employ the constituent-interchange model[12] (CIM), depicted in Fig. 1.

At small p_T, individual constituents of the proton are not probed incoherently, the scattering is "soft," and the inclusive cross section is an exponential in p_T^2. In the context of the CIM, the soft component corresponds to repeated iterations of the hard or "Born" term.[13] Both the hard and the soft component should contribute to scattering at all p_T^2, but, because of the power-law behavior, the hard term dominates at large p_T^2, and vice versa.

The uncertainty principle suggests that hadronic

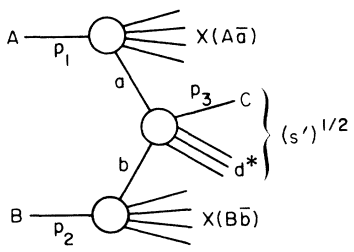

FIG. 1. CIM diagram for $A + B \to C + X$. The hadron-irreducible process $a + b \to C + d^*$ is hard and gives a momentum-balancing jet d^*. In general, particle C itself could be produced by bremsstrahlung in the irreducible subprocess $a + b \to c(c \to C + c') + d^*$.

constituents are probed for $p_T \gtrsim 1$ GeV/c, which is a rough definition of "large" p_T. Near $p_T \approx 1$ GeV/c there should be a transition region in which cross sections change from an exponential to a power-law dependence on p_T^2, and where other manifestations of the change from soft to hard scattering should occur.

As we discuss in the next section, we expect on general grounds that for fixed energy and missing mass the multiplicity associated with the hard component should be larger than that coming from the soft component, and therefore we anticipate a clear increase of the associated multiplicity in the transition region from the soft to the hard regime. In contrast, it is intrinsically difficult to differentiate between an exponential and a power law for the cross section in a small p_T range, so that to separate both contributing terms one can do a better job by analyzing the associated multiplicity rather than the single-particle distribution.

The paper is organized as follows. In Sec. II we discuss the expressions for the multiplicity associated with the hard and soft components. Multiplicity data from Fermilab and ISR are used to predict the hard and soft contributions to $\bar{n}_c$ at 28.5 GeV/c. In Sec. III, we parametrize the hard and soft components of the invariant cross section. Using cross-section data for small p_T we fix the soft term. Then, by fitting the BPV multiplicity data for $pp \to pX$ and $pp \to \pi^+ X$, we obtain the hard term and find the predicted total cross section (soft plus hard) to be in reasonable agreement with the data. Section IV contains a discussion of our results, and conclusions.

II. EXPRESSION FOR THE MULTIPLICITY

In our model, the associated mean total charged multiplicity for $p(p_1)+p(p_2) \to h(p_3)+X$ is given by the weighted average of the multiplicities coming from each component,

$$\bar{n}_c(p_3) f(p_3) = \bar{n}_s(p_3) f_s(p_3) + \bar{n}_h(p_3) f_h(p_3) . \tag{2.1}$$

Here $\bar{n}_s(p_3)$ [$\bar{n}_h(p_3)$] is the average charged multiplicity associated with the soft (hard) process, and

$$f_i(p_3) \equiv \left(E \frac{d^3\sigma}{d^3p} \right)_i \quad (i = s, h) \tag{2.2}$$

is the invariant single-particle distribution arising from soft or hard scattering, respectively. The invariant cross section is given by

$$f(p_3) \equiv E \frac{d^3\sigma}{d^3p} = f_s(p_3) + f_h(p_3) . \tag{2.3}$$

The multiperipheral model suggests[10] that the multiplicity associated with the soft component should depend only on M^2—in fact, this is one reason why the BPV multiplicity data are interesting. The M^2 dependence in the multiperipheral model is approximately logarithmic ($a + b \ln M^2$), with b close to unity,[14] so we take

$$\bar{n}_s(p_3) = a + \ln M^2 . \tag{2.4}$$

The parameter a is determined by assuming that at Fermilab energies[3] and for $M^2/s \lesssim 0.25$ and $p_T \lesssim 1$ GeV/c only the soft term contributes to $pp \to pX$ (there is no increase in the multiplicity with p_T at fixed missing mass in the data of Ref. 3). The naive parametrization[15]

$$\bar{n}_s(p_3) = 2 + \ln M^2 \tag{2.5}$$

gives a good description of the data of Ref. 3, as is shown in Fig. 2.

To derive an expression for the multiplicity associated with a hard process we refer to Fig. 1. The hard-process multiplicity is given by the sum of multiplicities from the irreducible (jet) process $\bar{n}_J$ and the remaining multiplicity $\bar{n}_R$,

$$\bar{n}_h(p_3) = \bar{n}_R(p_3) + \bar{n}_J(p_3) . \tag{2.6}$$

We assume, for simplicity, that the c.m. system for the irreducible collision in Fig. 1 coincides with the c.m. system for the pp collision. The subenergy in the irreducible process is denoted by $\sqrt{s'}$, so the energy remaining for particle production is $\sqrt{s} - \sqrt{s'}$. It is generally believed[16] that the asymptotic multiplicity in a given system of particles is determined principally by the energy

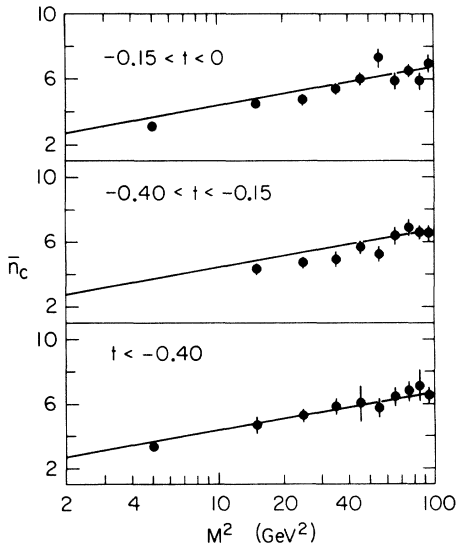

FIG. 2. Data from Ref. 3 for the average charged multiplicity $\bar{n}_c$ plotted versus M^2 for different t values. The solid lines represent the t-independent soft-scattering parametrization (2.5).

available, so we assume that the remaining particles should have a multiplicity depending on $(\sqrt{s}-\sqrt{s'})^2$ in the same way as $\bar{n}_s$ depends on M^2,

$$\bar{n}_R(p_3)=1+\ln(\sqrt{s}-\sqrt{s'})^2 . \tag{2.7}$$

We assume that $\bar{n}_J$ depends only on $|\vec{p}_3|$. This is based on the idea that the number of particles necessary to compensate the momentum of the trigger should be independent of angle (although the *cross section* for the irreducible process has an angular dependence). This picture is simple and plausible, but it is by no means compulsory.[17] It implies that, to explain multiplicity data, we shall use no supplementary p_T dependence beyond that coming from the transition from one mechanism to the other.

Combining (2.6) and (2.7), we have

$$\bar{n}_h(p_3)=1+\ln(\sqrt{s}-\sqrt{s'})^2+\bar{n}_J(|\vec{p}_3|) . \tag{2.8}$$

To determine the jet contribution, we note that at 90° at ISR energies the logarithm in (2.8) varies very little for $0\leq p_T\lesssim 4$ GeV/c (the opposite is true at Brookhaven energies), so that $\bar{n}_h$ depends on p_T only through $\bar{n}_J(|\vec{p}_3|)$. If we assume that $\bar{n}_c(p_3)=\bar{n}_h(p_3)$ for $p_T\gtrsim 1$ GeV/c, then the observation[18] that $\bar{n}_c$ rises approximately linearly with p_T at the rate of ≈ 0.5 charged particle/(GeV/c) means that

$$\bar{n}_J(|\vec{p}_3|)=a_1+0.5\,|\vec{p}_3| . \tag{2.9}$$

As $|\vec{p}_3|\to 0$, only one particle is needed in the jet to balance the momentum, and by isospin arguments its average $\bar{n}_c$ is approximately 0.7. Therefore $a_1\approx 1.7$, and

$$\bar{n}_J(|\vec{p}_3|)=1.7+0.5\,|\vec{p}_3| . \tag{2.10}$$

Substituting (2.10) in (2.8) we have

$$\bar{n}_h(p_3)=2.7+\ln(\sqrt{s}-\sqrt{s'})^2+0.5\,|\vec{p}_3| . \tag{2.11}$$

To calculate $\sqrt{s'}$ we assume that the particles in the jet are mostly pions, so that the energy associated with the jet is given by

$$E_J=\sum_i(|\vec{p}_i|^2+m_i^2)^{1/2}\approx\sum_i|\vec{p}_i| , \tag{2.12}$$

where the sum is over the jet particles. To estimate the sum in (2.12) we assume that the momenta of the particles comprising the jet are almost collinear with $-\vec{p}_3$. This implies that

$$\sum_i|\vec{p}_i|\approx|\vec{p}_3| , \tag{2.13}$$

so that the subenergy in the irreducible collision is

$$\sqrt{s'}\approx(|\vec{p}_3|^2+m_N^2)^{1/2}+|\vec{p}_3| . \tag{2.14}$$

Formula (2.14) must underestimate the jet energy, particularly for large values of $|\vec{p}_3|$ when the jet consists of a large number of particles. It corresponds to the neglect of the missing mass M' in the jet, so that in general

$$\sqrt{s'}=(|\vec{p}_3|^2+m_N^2)^{1/2}+(|\vec{p}_3|^2+M'^2)^{1/2} . \tag{2.15}$$

If, at large $|\vec{p}_3|$, M' should become appreciable, the argument of the logarithm in (2.11) would decrease more rapidly with increasing $|\vec{p}_3|$ than is suggested by (2.14). For example, if the jet multiplicity depends asymptotically on its invariant energy in the same way as other multiplicities do, we have, using (2.9),

$$\bar{n}_J(p_3)\approx\tfrac{1}{2}|\vec{p}_3|\approx\ln M'^2 ,$$

or

$$M'^2\approx\exp(\tfrac{1}{2}|\vec{p}_3|). \tag{2.16}$$

When $|\vec{p}_3|$ is large, this effect may cause a leveling-off of the rise in $\bar{n}_c$, although it should not be too important for $|\vec{p}_3|\lesssim 8.5$ GeV/c (i.e., $M'^2\lesssim|\vec{p}_3|^2$).[19]

When M^2 is small, say $M^2\lesssim 4$ GeV^2, we expect deviations from (2.5); similarly, (2.11) may not hold when $(\sqrt{s}-\sqrt{s'})^2\lesssim 4$ GeV^2.

Independent of any parametrization, we expect that

$$\bar{n}_h(p_3)\geq\bar{n}_s(p_3). \tag{2.17}$$

The reason is that the hard process correlates some of the produced particles into a jet. Therefore, more particles are needed to produce a given missing mass in the hard process than in the soft process. The inequality (2.17) is satisfied by (2.5) and (2.11) in their range of applicability. Near the phase-space boundary of the inclusive process, we expect that (2.17) should reduce to an approximate equality, because in that case kinematics constrains the soft process to have a jet-like momentum-balancing structure similar to that of the hard process. In this kinematic boundary region (2.11) does not hold since $\sqrt{s}-\sqrt{s'}\leq 1$ GeV.

For $pp\to\pi^+X$ the associated multiplicity is roughly 1.1 particles less than for $pp\to pX$ at the same p_T and missing mass.[5] Thus (2.5) and (2.11) should be reduced by 1.1 particles to describe $pp\to\pi^+X$,

$$\bar{n}_i^{\pi^+}(p_3)=\bar{n}_i^{p}(p_3)-1.1\quad(i=s,h). \tag{2.18}$$

This is qualitatively explained by the fact that the missing mass in $pp\to\pi^+X$ contains two nucleons. For example, if we assume that

$$\bar{n}_s^{\pi^+}(p_3)=a_2+\ln M^2 \tag{2.19}$$

and evaluate (2.19) at $M^2=4m_N^2$, we get

$$a_2=2-\ln(4m_N^2)\approx 0.75. \tag{2.20}$$

Comparing (2.5) and (2.19), we get

$$\bar{n}_s^{\pi^+}(p_3) \approx \bar{n}_s^p(p_3) - 1.25, \tag{2.21}$$

and for the hard term the result is

$$\bar{n}_h^{\pi^+}(p_3) \approx \bar{n}_h^p(p_3) - 1.22, \tag{2.22}$$

both in good agreement with (2.18).

III. CROSS SECTION AND COMPARISON WITH DATA

Before applying (2.1) to the BPV multiplicity data, we need to parametrize f_s and f_h. For the soft cross section for $pp \to pX$, we take a triple-Regge form,[20]

$$f_s^p(p_3) = \frac{2p_{\max}}{\pi\sqrt{s}}\left(s\frac{d^2\sigma}{dt\,dM^2}\right)_s = \frac{2p_{\max}}{\sqrt{s}}\left[\beta_{PPP}(t)\left(\frac{M^2}{s}\right)^{1-2\alpha_P(t)} + \beta_{RRP}(t)\left(\frac{M^2}{s}\right)^{1-2\alpha_R(t)} + \beta_{RRR}(t)\left(\frac{M^2}{s}\right)^{1-2\alpha_R(t)}(M^2)^{\alpha_R(0)-1}\right], \tag{3.1}$$

where $p_{\max}$ is the c.m. beam momentum. We do not include the diffractive scale-breaking PPR term because we do not expect it to be important in the kinematic region of interest to us ($M^2/s \gtrsim 0.1$ at Brookhaven energies). Our Pomeron trajectory is given by

$$\alpha_P(t) = 1 + 0.3t, \tag{3.2}$$

while the (effective) nondiffractive trajectory α_R reads[21]

$$\alpha_R(t) = 0.2 + 0.75t. \tag{3.3}$$

The triple-Regge couplings are taken to be exponentials in t,

$$\beta_i(t) = \beta_i e^{b_i t} \quad (i = PPP, RRP, RRR). \tag{3.4}$$

Formula (3.1) is known[21] to give a reasonably good description of data for $x_L \gtrsim 0.5$, where x_L is the longitudinal variable

$$x_L = \frac{p_L}{p_{\max}}. \tag{3.5}$$

We need, in addition, a parametrization of the soft term for $x_L \lesssim 0.5$. In the context of the BPV multiplicity data, $x_L \lesssim 0.3$ corresponds to large p_T values where, in our model, the hard term is dominant and the soft parametrization is unimportant.[22] For $0.3 \lesssim x_L \lesssim 0.5$ the soft term should be a smooth extrapolation of the soft cross section for $x_L \gtrsim 0.5$. The simplest way to ensure this is to take the triple-Regge formula (3.1) as the soft term in the region $0.3 \lesssim x_L \lesssim 0.5$. The use of other reasonable extrapolations in this region does not change our conclusions; therefore we keep the triple-Regge parametrization for all values of x_L.

The best place to fix the free parameters of (3.1) would be at values of p_T where we assume there is no hard term, that is, the 205-GeV/c data of Ref. 3, where there is no increase in the multiplicity with p_T at fixed missing mass. In addition to the 205-GeV/c data, in order to evaluate the RRR term we have taken the 24-GeV/c data of Ref. 23 for values of x_L corresponding to those of the BPV multiplicity data where there is no increase of $\bar{n}_c$.[21]

The fitted parameter values are

$$\begin{aligned} &\beta_{PPP} = 1.88 \text{ mb GeV}^{-2}, \quad b_{PPP} = 5.67 \text{ GeV}^{-2}, \\ &\beta_{RRP} = 47.1 \text{ mb GeV}^{-2}, \quad b_{RRP} = 1.75 \text{ GeV}^{-2}, \\ &\beta_{RRR} = 114.4 \text{ mb GeV}^{-2}, \quad b_{RRR} = 0.4 \text{ GeV}^{-2}. \end{aligned} \tag{3.6}$$

The resulting soft-scattering component is shown as the dashed lines with the 205-GeV/c data of Ref. 3 in Figs. 3(a) and 3(b), and with the 24-GeV/c and 29.7-GeV/c data of Refs. 23 and 25 in Fig. 4. Notice that in Fig. 4 we show our extrapolation for values of $x_L < 0.5$, as discussed in the preceding paragraph.

For $pp \to \pi^+ X$, the nucleon pole lies near the physical region, so we take[26]

$$f_s^{\pi^+}(p_3) = \frac{2p_{\max}}{\sqrt{s}}\beta_{NNP}(t)\left(\frac{M^2}{s}\right)^{1-2\alpha_N^*(t)}(m_N^2 - t)^{-1}, \tag{3.7}$$

where $\alpha_N^*(t)$ is an effective nucleon trajectory

$$\alpha_N^*(t) = \alpha_N + \alpha_N' t, \tag{3.8}$$

and $\beta_{NNP}(t)$ is an exponential in t,

$$\beta_{NNP}(t) = \beta_{NNP} e^{b_{NNP} t}. \tag{3.9}$$

By fitting the 24-GeV/c data[23] for $pp \to \pi^+ X$ for values of x_L where, as above, we believe there is no hard contribution,[24] with the parametrization (3.7) we get the dashed lines shown with the data in Fig. 5. The parameter values obtained from the fit are

$$\begin{aligned} &\alpha_N = -1.10, \quad \alpha_N' = 0.60 \text{ GeV}^{-2}, \\ &\beta_{NNP} = 9.23 \text{ mb}, \quad b_{NNP} = 0.50 \text{ GeV}^{-2}. \end{aligned} \tag{3.10}$$

For the hard contribution to scattering we use a form suggested by the CIM,[12]

$$f_h(p_3) = A(1 - x_R)^F (p_T^2 + m_0^2)^{-N}. \tag{3.11}$$

Here x_R is the radial variable,

$$x_R = |\vec{p}_3|/p_{\max}, \tag{3.12}$$

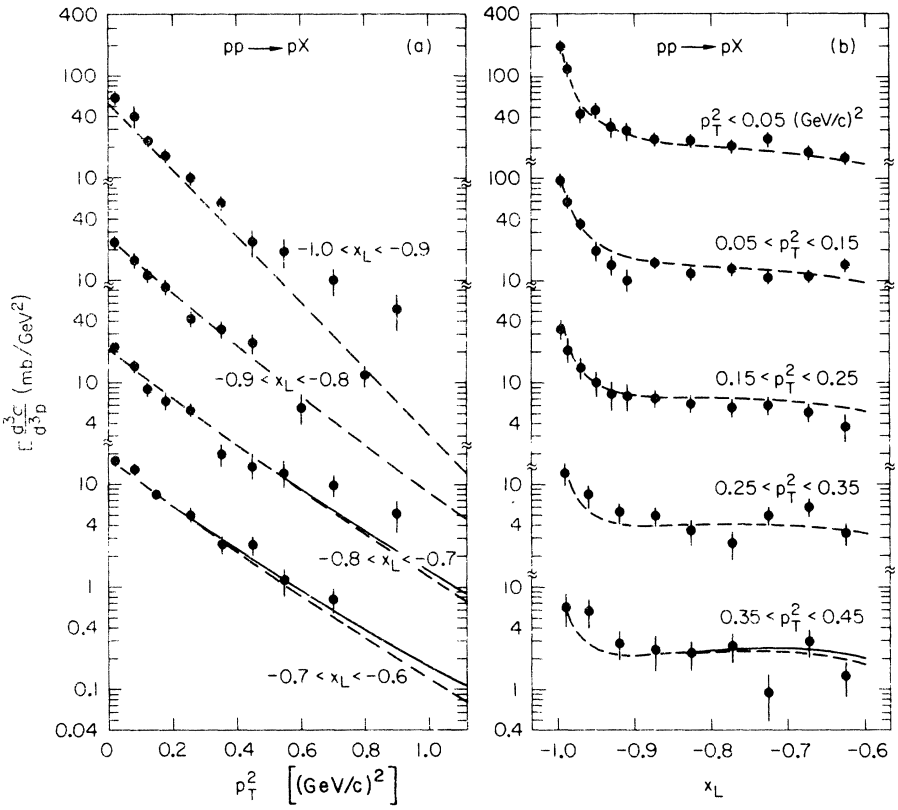

FIG. 3. Data for the invariant cross section for $pp \to pX$ from Ref. 3, (a) plotted versus p_T^2 for various fixed values of x_L, (b) plotted versus x_L for various fixed values of p_T^2. The dashed lines are the triple-Regge fit (3.1), and the solid lines are our predicted total (hard plus soft) invariant cross section in the region where it differs from the soft term.

and m_0^2 is a mass scale which may differ from process to process. In the CIM, $f_h(p_3)$ consists of a sum of terms such as (3.11) with definite values for F and N. We shall regard (3.11) as an effective hard term, summarizing the sum over a limited kinematic range.

According to (2.1), the hard component $f_h(p_3)$ can now be obtained by fitting the BPV data for $\bar{n}_c(p_3)$. In principle, we could use the expressions (2.5), (2.11), and (2.18) for $\bar{n}_s(M^2)$ and $\bar{n}_h(M^2)$, but instead we obtain $\bar{n}_s$ and $\bar{n}_h$ directly from the BPV data by assuming that, for fixed missing mass, the scattering is essentially pure soft for the lowest p_T values and pure hard for the highest p_T values. The values for $\bar{n}_s$ and $\bar{n}_h$ obtained by this method are given in Table I, and are seen to be in good agreement with the parametrizations (2.5), (2.11), and (2.18), also given in Table I. Since the multiplicity is given by the weighted average of the multiplicities of each component, the reader can check that with fixed hard and soft cross sections the resulting $\bar{n}_c$ is approximately the same for the empirical $\bar{n}_h$ and $\bar{n}_s$ as for the parametrized $\bar{n}_h$ and $\bar{n}_s$.

Thus, using the values given in columns 3 and 4 of Table I, together with expression (3.11), we have fitted (2.1) to the BPV data for $pp \to pX$. We allowed the normalization parameter A to vary free of constraint and we chose the parameters N, F, and m_0^2 to be consistent with values obtained by fitting the CIM to data at Fermilab energies.[12] The result is shown as the solid lines in Fig. 6(a), with

$$A = 1.26 \times 10^3 \text{ mb GeV}^8, \quad m_0^2 = 3.0 \text{ GeV}^2, \quad F = 3, \quad N = 5. \tag{3.13}$$

The fit is not particularly sensitive to changes in the parameter values of $\Delta F \approx \pm\frac{1}{2}$, $\Delta N \approx \pm\frac{1}{2}$, and $\Delta m_0^2 \approx \pm 1$ GeV^2. The sharpness of the rise in $\bar{n}_c$ in Fig. 6(a) is controlled by m_0^2 and N; increasing m_0^2 and/or decreasing N produces a sharper rise over a shorter interval in p_T. The location of the rise as a function of M^2 is controlled by F. These features are seen to be well described by our model.

At this juncture, we have determined both the soft term (3.1) and the hard term (3.11) for $pp \to pX$. The predicted total invariant cross section, given by (2.3), is shown as the solid lines in Figs. 3(a), 3(b), and 4. For $p_T \leq 0.35$ GeV/c the soft component (dashed lines) dominates the cross section when $x_L \geq 0.3$, while the hard component begins to become important for $p_T \gtrsim 0.65$ GeV/c, and con-

stitutes over 90% of the cross section at $p_T = 1.6$ GeV/c. Evidently, the soft component alone is insufficient to describe the cross section at large p_T, while the addition of the hard component brings the resulting cross section into much better agreement with the data. Although the hard component becomes dominant in a relatively short interval of p_T, as is shown by Fig. 6(a), the invariant distribution, when plotted versus p_T^2 at fixed x_L, shows little evidence of a break; the transition from soft to hard as p_T increases is smooth in the cross section.

The BPV data show that the rise in $\bar{n}_c$ shifts to smaller values of p_T for increasing M^2, which must be interpreted in our model as a corresponding change in the p_T value where hard scattering becomes important. We note in this connection that, although the multiplicity data do not imply hard scattering for $p_T < 0.4$ GeV/c (see Fig. 6), with our parametrization the hard component is appreciable when $x_L \lesssim 0.3$ even for $p_T = 0.15$ (see Fig. 4). It is difficult to understand how the hadronic constituents could be probed at such small transverse momentum. Notice, however, that at

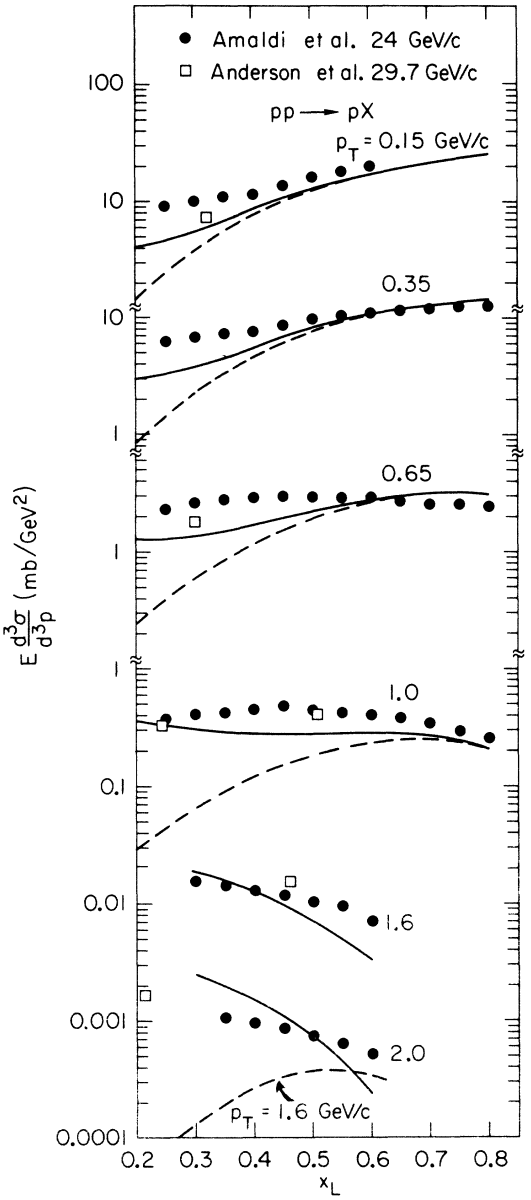

FIG. 4. Data for the invariant cross section for $pp \to pX$ from Refs. 23 (circles) and 25 (squares) plotted versus x_L for various values of p_T. The dashed lines are the triple-Regge formula (3.1), and the solid lines are our prediction for the total (hard plus soft) invariant cross section.

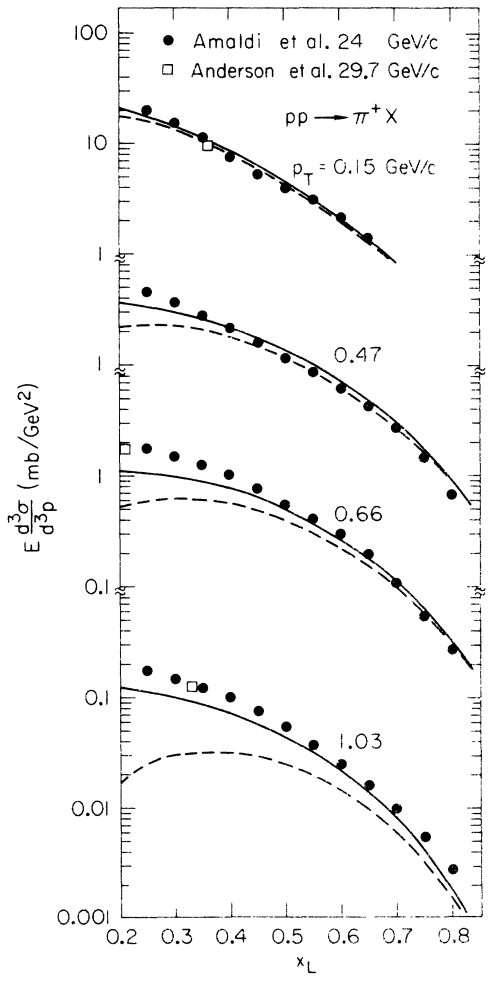

FIG. 5. Data for the invariant cross section for $pp \to \pi^+ X$ from Refs. 23 (circles) and 25 (squares) plotted versus x_L for various values of p_T. The dashed lines are the formula (3.7), and the solid lines are our prediction for the total (hard plus soft) invariant cross section.

24 GeV/c for $p_T = 0.15$ GeV/c and $x_L \leq 0.3$ GeV/c, we have $\epsilon = M^2/s \geq 0.64$ (or $|\vec{p}_3| \leq 0.98$), whereas we have fixed our parametrization of the hard term for $\epsilon < 0.54$ (see data in Fig. 6). In the CIM the effective parameters N and F may depend on p_T and ϵ, corresponding to different dominating terms in different kinematic regions. A possibly more important correction to our results is the inclusion of the expected angular dependence in the hard term, which we have neglected in (3.11). This correction should be most important at small $|\vec{p}_3|$, where a small change in p_T corresponds to a large change in the angle (we have fixed our parametrization using multiplicity data for $|\vec{p}_3| \geq 1.5$ GeV/c).

For $pp \to \pi^+ X$ we again use the values of $\bar{n}_s$ and $\bar{n}_h$ given in columns 3 and 4 of Table I to fit (2.1) to the BPV data. Again, F, N, and m_0^2 were chosen to be consistent with fits to data at Fermilab energies, and A was allowed to vary freely. The resulting parameter values are

$$A = 3.6\times10^2 \text{ mb GeV}^8, \quad m_0^2 = 2.0 \text{ GeV}^2, \quad F = 4, \quad N = 5, \tag{3.14}$$

and the fit is shown as solid lines with the data in Fig. 6(b). The invariant cross section (2.3) for $pp \to \pi^+ X$ is displayed as the solid lines in Fig. 5. Our remarks concerning the fits to the $pp \to pX$ data carry over for the $pp \to \pi^+ X$ case.

The striking similarity in the multiplicity data for p and π^+ triggers is at least partially understood in our model. For fixed missing mass, $\bar{n}_h^p - \bar{n}_h^{\pi^+} \approx \bar{n}_s^p - \bar{n}_s^{\pi^+}$ because the same mechanism which reduces the yield of particles when a π^+ is the trigger operates in both the hard and soft processes. Therefore, for fixed M^2 the π^+ data should show a rise equal in magnitude to that for the proton data. That the location of the rise should be the same for π^+ as for p is not *a priori* clear, although one expects the constituent structure to manifest itself at roughly the same value for all processes.

TABLE I. Mean charged multiplicities for soft and hard components.

	M (GeV)	Empirical multiplicity		Parametrizations (2.5), (2.11), (2.18)	
		$\bar{n}_s$	$\bar{n}_h$	$\bar{n}_s$	$\bar{n}_h$
$pp \to pX$	1.66	2.75	2.75	3.01	a
	2.56	3.75	4.45	3.88	a
	3.57	4.40	5.00	4.54	5.19
	4.56	5.00	5.80	5.03	5.90
	5.47	5.45	6.35	5.40	6.31
	6.15	···	6.70	5.63	6.48
$pp \to \pi^+ X$	4.56	3.90	4.90	3.93	4.80
	5.47	4.40	5.30	4.30	5.21
	6.15	5.00	5.70	4.53	5.38

[a] The parametrization (2.11) is not applicable for $M = 1.66$ or 2.56 GeV because $\sqrt{s} - \sqrt{s'} < 1$ GeV.

IV. DISCUSSION AND CONCLUSION

In the present work we have investigated the possibility that the concept of hard scattering, which has been applied to high-p_T cross section data by many authors, may have interesting, observable consequences for the associated multiplicity. We have investigated whether the steplike behavior of the Brookhaven-Purdue-VPI multiplicity data can be attributed to the onset of hard scattering, and have found that such an interpretation is consistent with experiment. At the present stage, our parametrization gives a general description of our two-component mechanism without specifying all the details. For instance, the transition from exponential to power-law behavior in the cross section is incorporated in the model without reference to deviations from a single exponential for the soft term, angular dependence of the hard term, etc. In fact, the relative weights are well tested only in the transition region for the multiplicity;

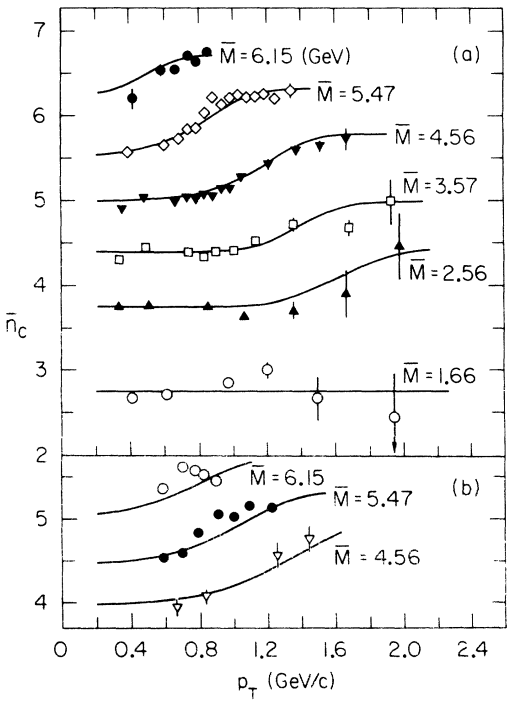

FIG. 6. Total mean charged multiplicity plotted versus p_T for various fixed values of the average missing mass $\overline{M}$. The data are from Ref. 5 and the solid lines are our fits. (a) $pp \to pX$, (b) $pp \to \pi^+ X$.

at low and high p_T the scattering is (essentially) either pure soft or pure hard, respectively.

Support for the dominance of hard scattering at ISR energies comes from the observation[1] that the rise in multiplicity with increasing p_T is associated with particle production in a broad region in the hemisphere of phase space opposite to that of the trigger. The rise is confined to a range of approximately 120° in azimuthal angle ϕ centered at $\phi = 180°$, which is consistent with our picture of a momentum-balancing jet. Similarly, the rise in $\bar{n}_c$ observed by the BPV collaboration appears to come from the opposite hemisphere.[4] Furthermore, the fact that the relative contributions of the n-prong cross sections all exhibit a significant change at the same value of p_T for fixed missing mass[4] suggests the onset of a new dynamical mechanism at this value of p_T. Finally, at 28.5 GeV/c the distribution of π^-'s associated with a trigger proton has been measured.[27] No increase in the width of the momentum distribution normal to the scattering plane is observed; such behavior is difficult to reconcile with fireball models,[1] and is consistent with our scheme.

A test of our model would be the observation at Fermilab and ISR energies of steplike behavior for $\bar{n}_c$ at fixed missing mass. The multiplicities below and above the rise should be consistent with (2.5) and (2.11), respectively, provided that M^2 is not too small and $|\vec{p}_3|$ is not too large. If the scale-breaking terms of the soft component are not too large our model predicts that, for a given ϵ, the step should be located at approximately the same p_T value as is seen at 28.5 GeV/c; in our model the variable ϵ, rather than M^2, determines the location of the rise in $\bar{n}_c$. For instance, if at Fermilab it is difficult[3] to obtain data for transverse momenta greater than ~1 GeV/c, it should be sufficient to take $M^2 \approx 200$ GeV^2 ($\epsilon \approx 0.5$) to observe the rise in multiplicity. This value of ϵ corresponds to a missing mass of 5.47 GeV at Brookhaven energies, where the rise occurs for $0.5 \lesssim p_T \lesssim 1.0$ GeV/c. We note, however, that this prediction should be modified to take into account the (imperfectly known) energy dependence of the effective parameters N and F.

According to our picture, changes in the invariant cross section occur in the transition from soft to hard scattering. It would seem, however, that changes in the behavior of the associated multiplicity may be one of the sharpest signals of a fundamental transition in the dynamics of particle production.

ACKNOWLEDGMENTS

We thank J. D. Bjorken, R. Blankenbecler, S. J. Brodsky, R. O. Raitio, G. A. Ringland, and D. Sivers for helpful discussions. Thanks are due to S. J. Brodsky and D. Sivers for reading the manuscript. We are indebted to W. N. Schreiner for providing us with the BPV data in tabular form. One of us (J. L. A.) wishes to acknowledge the warm hospitality of Professor S. D. Drell and SLAC.

---

*Work supported in part by the U. S. Energy Research and Development Administration.

†On leave of absence from Departamento de Física Teorica, Universidad de Zaragoza, Spain. Work supported in part by Program for Cultural Cooperation between the United States and Spain.

‡National Research Council of Canada Postdoctorate Fellow.

[1]These results are discussed in the following review articles: S. D. Ellis and R. Thun, CERN Report No. CERN-TH-1874 (unpublished); P. V. Landshoff, in *Proceedings of the XVII International Conference on High Energy Physics, London, 1974,* edited by J. R. Smith (Science Research Council, Rutherford Laboratory, Chilton, Didcot, U.K., 1974), p. V-57; J. W. Cronin, in proceedings of the Summer Institute on Particle Physics, SLAC, 1974, edited by M. C. Zipf [SLAC Report No. SLAC-179, 1974 (unpublished)].

[2]G. Finocchiaro *et al.*, Phys. Lett. 50B, 396 (1974); G. Finocchiaro *et al.*, R. Kephart *et al.*, F. Büsser *et al.*, papers submitted to the XVII International Conference on High Energy Physics, London, 1974 (unpublished).

[3]J. Whitmore, S. J. Barish, D. C. Colley, and P. F. Schultz, Phys. Rev. D 11, 3124 (1975).

[4]A. Ramanauskas *et al.*, Phys. Rev. Lett. 31, 1371 (1973); E. W. Anderson *et al.*, paper submitted to the XVII International Conference on High Energy Physics, London, 1974 (unpublished).

[5]E. W. Anderson *et al.*, Phys. Rev. Lett. 34, 294 (1975).

[6]S. Choudhury, Nuovo Cimento Lett. 11, 530 (1974).

[7]A. S. Kanofsky and K. F. Klenk, Phys. Rev. Lett. 31, 1323 (1973).

[8]L. J. Gutay and P. Suranyi, Phys. Rev. D 9, 2501 (1974).

[9]A. P. Contogouris, J. P. Holden, and E. N. Argyres, Phys. Lett. 51B, 251 (1974).

[10]C.-F. Chan and F. C. Winkelman, Phys. Rev. D 10, 3645 (1974). This model is applied to 205-GeV/c data for $\bar{n}_c$ in $\pi^- p \to pX$. Since $p_T \lesssim 1$ GeV/c, and $M^2 \lesssim 170$ GeV^2, neglect of the hard component is probably justified here.

[11]See the reviews of Ellis and Thun (Ref. 1) and Landshoff (Ref. 1) for discussions of hard-scattering models.

[12]R. Blankenbecler, S. J. Brodsky, and J. F. Gunion, Phys. Lett. 42B, 461 (1972); R. Blankenbecler and S. J. Brodsky, Phys. Rev. D 10, 2973 (1974). For reviews of the CIM and references see R. Blankenbecler, in proceedings of the Summer Institute on Particle Physics, SLAC, 1974, edited by M. C. Zipf [SLAC Re-

port No. SLAC-179, 1974 (unpublished)]; S. J. Brodsky, *ibid.*; J. F. Gunion, in *Proceedings of the XVII International Conference on High Energy Physics, London, 1974,* edited by J. R. Smith (Ref. 1), p. I-125; D. Sivers, Ann. Phys. (N.Y.) 90, 71 (1975); D. Sivers, R. Blankenbecler, and S. J. Brodsky, SLAC Report No. SLAC-PUB-1595, 1975 (unpublished).

[13]R. Blankenbecler, S. J. Brodsky, J. F. Gunion, and R. Savit, Phys. Rev. D 8, 4117 (1973); 10, 2153 (1974).

[14]W. R. Frazer *et al.*, Rev. Mod. Phys. 44, 284 (1972); G. F. Chew and A. Pignotti, Phys. Rev. 176, 2112 (1968).

[15]Here we include the trigger proton in $\bar{n}_s$.

[16]See for instance E. L. Berger, in proceedings of Ecole d'Eté de Physique des Particules, Gif-sur-Yvette, France, 1973 (unpublished).

[17]S. D. Ellis and M. B. Kislinger, Phys. Rev. D 9, 2027 (1974).

[18]See for instance Cronin, Ref. 1.

[19]In our model, it is difficult to understand the rather sharp dropoff of $\bar{n}_c$ in the data of Ref. 2 at the highest values of p_T. One needs more data to be sure that this behavior is a physical effect and is not produced by a loss of events.

[20]C. E. DeTar, C. E. Jones, F. E. Low, J. H. Weis, J. E. Young, and C.-I Tan, Phys. Rev. Lett. 26, 675 (1971); G. F. Chew and A. Pignotti, in proceedings of the NAL 1968 Summer Study (unpublished), Vol. 3; L. Caneschi and A. Pignotti, Phys. Rev. Lett. 22, 1219 (1969); D. Silverman and C.-I Tan, Phys. Rev. D 2, 233 (1970); R. P. Feynman, in *High Energy Collisions,* edited by C. N. Yang *et al.* (Gordon and Breach, New York, 1969). For recent triple-Regge analyses of data, see D. P. Roy and R. G. Roberts, Nucl. Phys. B77, 240 (1974); R. D. Field and G. C. Fox, *ibid.* B80, 367 (1974).

[21]For references to triple-Regge fits employing effective trajectories, see D. W. G. S. Leith, in proceedings of the Summer Institute on Particle Physics, SLAC, 1974 (Ref. 12).

[22]The 6.15-GeV data are an exception; they have $x_L \lesssim 0.3$ for all values of p_T. Therefore, we do not include these data in the fit to the multiplicity, although we show our prediction in Fig. 6.

[23]U. Amaldi *et al.*, Nucl. Phys. B86, 403 (1974).

[24]The 24-GeV/c data were fitted in the following kinematic range, where, by inspection of the BPV multiplicity data, we expect that the soft term should dominate the cross section (p_T in GeV/c):

(i) $pp \to pX$; $p_T = 0.15$, $x_L \geq 0.45$; $p_T = 0.35$, $x_L \geq 0.55$; $p_T = 0.65$, $x_L \geq 0.60$; $p_T = 1.0$, $x_L \geq 0.75$;

(ii) $pp \to \pi^+ X$; $p_T = 0.15$, $x_L \geq 0.50$; $p_T = 0.47$, $x_L \geq 0.60$; $p_T = 0.66$, $x_L \geq 0.65$; $p_T = 1.03$, $x_L \geq 0.75$.

As we do not require a detailed fit to these data, we have taken points at intervals of $\Delta x_L = 0.05$ and have given them $\pm 10\%$ errors.

[25]E. W. Anderson *et al.*, Phys. Rev. Lett. 19, 198 (1967).

[26]E. L. Berger, Ph. Salin, and G. H. Thomas, Phys. Lett. 39B, 265 (1972).

[27]T. S. Clifford *et al.*, Phys. Rev. Lett. 34, 978 (1975).